Green Synthesis of Silver Nanoparticles for Its Usage as an Antimicrobial Agent

Noha M. Sorour [1], Asmaa Elnady[2], and Rateb N. Abbas [2*]

[1] Department of Industrial Biotechnology, Genetic Engineering and Biotechnology Research Institute, University of Sadat City.
[2] Department of Microbial Biotechnology, Genetic Engineering and Biotechnology Research Institute, University of Sadat City.

***Corresponding author: Rateb Nabil Abbas**
Department of Microbial Biotechnology, Genetic Engineering and Biotechnology Research Institute (GEBRI), University of Sadat City, Sadat City, Egypt, 22857/79
Tel.: +2-01154114555
Fax: +2-0482601266
E-mail address: **rateb.youssef@gebtri.usc.edu.eg**

ABSTRACT

Silver nanoparticles (AgNPs) were biosynthesized using aqueous extract of Citrus japonica (Kumquat) and Candida tropicalis culture supernatant. AgNPs were characterized using FTIR, UV-Vis, TEM, XRD, DLS, and EDAX. XRD confirmed the crystalline nature with four characteristic peaks at 2Ɵ values corresponding to Ag-nanocrystals. TEM showed spherical-shaped AgNPs with average diameter of 4-20 nm. FTIR verified the presence of different bio-functional groups, such as, N-H, C-N, O-H, C-H, C-O-C, C=O, and C-NH_2 acting as stabilizing/reducing agents for AgNPs. The biosynthesized AgNPs exhibited excellent biocidal activity against some pathogenic Gram-positive, Gram-negative bacteria, and Yeast. MIC and MBC of biosynthesized AgNPs were determined using resazurin microtiter-plate assay. Biosynthesized AgNPs by C. tropicalis exhibited MBC of 12, 24,24, and 48 µg/mL against E. coli, Candida sp., K. pneumonia, and L. monocytogenes, respectively. The MBC of Kumquat-AgNPs were 48 µg/mL against (E. coli, K. pneumonia, Candida sp.), and 195 µg/mL against L. monocytogenes. SEM micrographs showed complete cell destruction of K. pneumonia and L. monocytogenes after 6hof treatment with MBC values. C. tropicalis-AgNPs exhibited better anticancer effect than Kumquat-AgNPs with IC_{50} of 59.5 and 87.5 µg/mL, respectively, on Hep-G2cell lines. However, Kumquat-AgNPs proved less toxic than C. tropicalis-AgNPs towards normal cell lines with IC_{50} values >300 and 69.9 µg/mL, on Human Skin Fibroblast, and 68.41 and 28.43 µg/mL, on Blood Lymphocytes, respectively. Detected IC_{50}were higher than the MBC values of biosynthesized AgNPs against studied pathogens, thus, could be recommended to apply the mas powerful antimicrobial bioagent.

Keywords: Green synthesis, Kumquat, Silver nanoparticles, Antimicrobial, Candida tropicalis, Gram-positive, Gram-negative, anticancer.

1. INTRODUCTION

The extensive practical applications of nanoparticles (NPs) are in continuous increase due to their unique excellent properties including, optical, electrical conductivity, physicochemical, catalytic, stability, and magnetic behavior ***(Singla et***

special issue for the second international conference on genetic engineering & biotechnology "biotechnology and artificial intelligence towards sustainable development" (baisd-2019), 25-26th december, 2019, alexandria, egypt.

al.,2016; Mourdikoudis et al.,2018). *The* primary challenge is to develop specific methodologies in order to synthesize NPs of distinct size, particular shape, structure, controlled dispersity, and safe making them more compatible candidates in biomedical, environmental, and biotechnological applications **(Morones et al., 2005).**

On the other hand, there is a tremendous motivation to create novel bactericides because the emergence of new bacterial strains that are resistant to existing antibiotics has become a significant issue. AgNPs has been used in the medical sector as ointments to avoid infections of burn and *wounds* ***(Pourali and Yahyaei, 2016).*** *With* over 200 marketed applications, AgNPs are currently one of the most extensively employed nanomaterials. They are used in anti-microbial coatings, medical devices, molecular diagnostics and photonic devices, sensors, textiles, home water purifiers, cosmetics, household appliances, pastes, and fillers. ***(Zhang et al., 2016)***.

In general, physicochemical methods of synthesis aren't recommended since they sometimes involve hazardous chemical reagents, intense energy consumption, and generate toxic end-products that affect the human health and environment ***(Srikaret al., 2016)***.Consequently, there is a growing need for the developing of green eco-friendly protocols to produce nanomaterials that would avoid these drawbacks ***(Moroneset al., 2005;Shamailaet al., 2016***).Biological methods have smooth way for "greener synthesis" of NPs and they offer enhanced handling and control for crystal growth and stabilization ***(Shamaila et al., 2016).*** In this regard, the use of environmentally benign methods like microorganisms or plant extracts for the biosynthesis of AgNPs provide simple/viable methods alternative to physico-chemical processes with eco-friendly, cost-effective, safe and compatible benefits for biomedical, pharmaceutical and other industrial applications ***Ahmed et al., 2016).*** Therefore, the purpose of the present study is to apply green principles for AgNPs biosynthesis, using two different biological agents namely, Candida tropicalis yeast and Citrus japonica(Kumquat) extract. Characterization of the produced AgNPs has been investigated using different methods. A comparative analysis of the antimicrobial efficacy of biosynthesized AgNPs against some multidrug-resistant pathogenic strains was investigated, also the cytotoxic effect of the produced AgNPs was assessed in vivo on different normal and cancerous cell lines.

2. MATERIALS AND METHODS

2.1. Chemicals and microorganisms

AgNO3 was obtained from Sigma-Aldrich, USA. Culture nutritional components as Peptone, Glucose, Starch, Yeast and Malt extracts were purchased from Lobal Chemie, India. Throughout the experiment, double-distilled water that has been sterilised was used. The compounds were procured from Sigma/Aldrich in the United States, and all cell culture supplies for cytotoxicity testing were obtained from CambrexBioScience (Copenhagen, Denmark). Locally, other chemicals were purchased. Gram-positive bacteria (Staphylococcus aureus, Bacillus subtilis, and Listeria monocytogenes), gram-negative bacteria (Escherichia coli, Klebsiella pneumonia, and Acinetobacter baumannii), and Candida species were collected from El-Mabaret Educational Hospital, Alexandria, Egypt.

2.2. Preparation of Kumquat aqueous peel extract (KaqPE)

Fresh and healthy Citrus japonica fruits were collected from the local market of Sadat City, Menufyia governorate, Egypt. Fruits peels were collected, washed well, cut into small pieces and dried at 40oC in the oven until complete dryness then

powdered. Five grams of powdered C. japonica fruit peel were combined with 50mL of distilled water, and the mixture was cooked in a water bath for 15 min at 50ºC to create the aqueous extract (**Reenaa and Menon, 2017**). The KaqPE was filtered using Whatmann filter paper No. 1, then through a 0.45 um syringe filter, and then it was kept at 4°C for further use.

2.3.Preparation of Candida tropicalis cell free supernatant

C. tropicalis was kindly provided by Dr. Ashraf Elbaz, Professor of Microbiology, GEBRI, University of Sadat City, Egypt (El-Baz et al., 2011). The strain was grown on Wickerham's medium (Peptone 0.5%, Dextrose 1%, Yeast extract 0.3%, Malt extract 0.3%, Agar 2%, pH adjusted to 7.0) for 48 h at 28oC and maintained at 4oC for further use. C. tropicalis was grown in 250 mL-Erlenmeyer flask incubated in a rotary shaking incubator (New Brunswick, CA) at 150 rpm and 28oC for 48 h. After incubation, the culture broth was centrifuged for 15 min at 6000 rpm and the supernatant was collected and used for the biosynthesis.

2.4. Biosynthesis of AgNPs

Five mL of KaqPE was added separately to two different reaction vessels containing 50 mL of 1mM AgNO3.The first reaction vessel was incubated at 150 rpm in rotatory shaker in darkness at room temperature. The other one was stirred at 60oC using hot plate magnetic stirrer for one h. KaqPE as well as AgNO3 solution were kept as control.

Also, AgNPs was biosynthesized using C. tropicalis using equal volumes of AgNO3(1 mM)and C. tropicalis cell free supernatant incubated for 24 h with 150 rpm in darkness at room temperature. The effect of the Ag+ ions concentration was examined by varying the AgNO3 concentration (0.5-3 mM). To study the effect of temperature on AgNPs synthesis, the reaction mixtures containing 1 mM AgNO3were incubated at different temperatures (30, 45 and 60oC) for 24 h in rotatory shaker with150 rpm in darkness. Incubation time effect was evaluated after (12, 24, 48, and 72 h). The effect of pH on AgNPs biosynthesis was studied by adjusting the pH of the reaction at (2, 4.5, 7, 8, 9, 9.7, 10, and 11) incubated at 30oC in darkness. Control experiments were mixedAgNO3 solution and uninoculated media to check the role of yeast strain in biosynthesis. All experiments were carried out in triplicates and the reduction of Ag+ ions was examined by color change.

2.5. Characterization of AgNPs

During the biosynthesis, AgNPs formation was monitored using Shimadzu-T80 spectrophotometer (China) by sampling 2 mL of the produced AgNPs colloidal solution in a quartz cuvette and scanned at 300 to 700 nm. The morphology and particle size diameter were characterized by TEM using JEOL JEM 1400 instrument. The crystalline nature was investigated by X–ray diffraction (XRD) using (Bruker D2-Phaser diffractometer, 2nd *Generation)*, operating at 0.5 mA/50 kV, with a Cu anode radiation in 10°-70° angular range using continuous scanning 2Ɵ-mode. Particle size distribution of NPs was analyzed using a Nano-Zeta Sizer (Nano ZS, ZEN 3600, Malvern Nano, UK). Surface functional groups were identified using FTIR spectrum recorded byFTIR spectrometer 8000 series in the region of 4,000-400 cm-1. The metallic nano-morphology and the chemical composition of produced AgNPs was investigated by Energy Dispersive X-ray Spectroscopy (EDAX) measurement using JEOL JSM-6100 SEM at 20 kV.

2.6. Antimicrobial activity

2.6.1. Preparation of bacterial strains

The disc diffusion assay was used to test the antibacterial activity of the generated AgNPs against several Gram-positive (S. aureus, B. subtills, and L. monocytogenes), Gram-negative (E. coli, K. pneumonia, and A. baumannii) bacteria, as well as Yeast (Candida sp.). Except for L. monocytogenes, which was cultured on brain heart infusion medium (Oxoid), all bacterial strains were grown in Nutrient broth. Candida species were grown in Wickerham media. Fresh inoculum suspensions were made by selecting colonies cultivated at 37°C for 24 h and suspending them in 5 mL of sterile saline (0.9% w/v). Bacteria's and yeast's optical densities were corrected to the 0.5 McFarland standard of 1x108 CFU/mL and 1x106 CFU/mL, respectively (Andrews, 2001).

2.6.2. Disc diffusion assay

Pathogens inocula were spread on agar plates containing appropriate medium using a sterile cotton swab. Sterile discs (Hi-media) were saturated with 40 µL of two-folds serially diluted concentrations of AgNPs (0.39-25 mg/mL) prepared in 5% DMSO, sonicated for 5 min and placed on the agar surface. Discs saturated with C. tropicalis culture supernatant, KaqPE, and DMSO were used as a negative control, and standard Ceftriaxone antibiotic (30 µg/disc) was used as a positive control. The plates were placed at 4°C for 30 min to allow diffusion of NPs onto agar media. Inoculated plates were incubated at 37°C for 24 h. After incubation, the inhibition zones diameter was measured in mm and MIC was calculated as the lowest concentration of AgNPs that produced an inhibition zone after 24 h (Valgas et al., 2007).

2.6.3. MIC and MBC determination using resazurine microdilution assay

Resazurin dye was as an indicator for bacterial survival where color change from purple, to pink and colorless. 0.02% (w/v) resazurin solution was prepared according to Loo et al. (2018) method. The mixture was then filtered using 0.22 µm syringe filter and kept in dark at 4°C for 2 weeks. For the broth microdilution test (CLSI, 2012), the MIC of AgNPs was performed in 96-well microtiter plates. The microbial inocula were adjusted equivalent to 0.5 McFarland standard as mentioned above. Two-folds serially diluted concentrations of biosynthesized AgNPs (0.012-12.5 mg/mL) were prepared in 5% DMSO, sonicated for 5 min and used immediately.

For the MIC assay, 100 µL of each AgNPs concentration was added in each well and diluted with 100 µL of microbial inoculums to give two-folds concentrations ranging from 6.25 to 0.006 mg/mL. Column 1 of the microtiter plate had the highest concentration of AgNPs and column 11 had the lowest concentration. Positive control wells in column 12 were prepared with medium and bacterial suspension. Row 8 served as negative control (medium and diluted AgNPs).30 µL of resazurin solution was added to each well of the microtiter plates and incubated at 37oC for 24 h in dark.

If any color shift was noticed, pink/colorless indicates the presence of bacteria while blue/purple color shows the absence of bacteria. The MBC was defined as the lowest concentration that completely kills the bacteria, and the MIC value was obtained at the lowest concentration of AgNPs that inhibits the pathogen's development while keeping the color blue (Loo et al., 2018). For the MBC assay, all pathogens were plated onto nutrient agar plates with the exception of L. monocytogenes and Candida sp., which

were plated on brain heart infusion and Wickerhams media, respectively. The MBC value was calculated using the lowest AgNPs concentration that showed no discernible growth after 24 hours of incubation of the inoculated plates.

2.7. EMimaging of treated bacterial cells

The bacterial cells that had been treated with AgNPs were examined using scanning electron microscopy (SEM), as described by Fischer et al. (2012).18 h oldL. monocytogenes and K. pneumonia(10 mL) cultures were treated with AgNPs at their detected MBC and incubated for 3 h and 6 h. Treated bacterial pellets were collected by centrifugation and the culture supernatants were discarded. Treated bacterial cells were washed by phosphate buffer (pH7.0) to remove excess AgNPs precipitated on cells. Washed cells were fixed using fixative solution containing: 1% glutaraldehyde, 4% paraformaldehyde in sodium-cacodylate (0.1 M) at 4oC for maximum 24h. Samples were then post-fixed in 2% OsO4 in phosphate saline buffer (pH7.4) at 4ºC for 2 h, washed and dehydrated through series exposure to ethanol and blown dry using N2. Finally, samples were fixed using carbon paste on an AL-stub and coated with gold up to 400 Åthickness. Micrographs were captured using Jeol JSM-5300 SEM, at Faculty of Science, Alexandria University, Alexandria, Egypt.

2.8. Cytotoxicity and anticancer assessment

Cytotoxicity of biosynthesized AgNPs against Hepatocellular carcinoma (Hep-G2), Lung cancer (A549) cell lines, and normal Human Skin Fibroblast (HSF) celllines was performed by sulforhodamine B protein (SRB)at concentration (0.03-300 µg/mL) and on Peripheral Blood Lymphocytes by MTT assay at concentration (48 to 500 µg/mL).

2.8.1. Sulforhodamine B protein

Nawah Scientific Inc. provided the HepG2, A549, and HSF (Mokatam, Cairo, Egypt). At 37°C, cells were kept in Dulbecco's Minimum Essential Medium (DMEM) supplemented with streptomycin (100 mg/mL), penicillin (100 U/mL), and 10% heat-inactivated fetal bovine serum in humidified CO2 (5% v/v). 96-well plates with 100 µL aliquots of cell suspension (5x103 cells) inside were then cultured in DMEM medium for 24 h. Another aliquot of 100 mL of medium with various AgNPs concentrations was used to treat the cells. After 72 h of exposure, treated cells were fixed by removing the medium and soaking the cells in 150 L of 10% TCA for 1 hour at 4°C. After the TCA solution was withdrawn, distilled water was used to wash the cells five times. At room temperature, aliquots of a 70 µL SRB solution (0.4% w/v) were added and incubated for 10 min in the dark. Plates were cleaned with 1% acetic acid and let to dry naturally the following day. The protein-bound SRB stain was then dissolved in 150 µL of TRIS (10 mM), and the absorbance was determined using a BMGLABTECH®-FLUO star Omega microplate reader (Ortenberg, Germany) based on the Skehan et al. (1990) technique at 540 nm.

2.8.2. MTT assay

Fresh blood samples totaling 20 mL were taken, and the normal blood lymphocytes were separated using the Kizhakeyil et al. (2019) method. Centrifuging lymphocyte cell suspension at 2000 rpm for 10 min, washing the cells, and then suspending them in unfinished RPMI-1640. Trypan blue stain (Sigma) was used to examine cell viability, and it showed that it was above 90%. RPMI-1640 supplemented with 10%

FBS was used to culture cells (2.5X105 mL) in triplicates in flat-bottom 96-well tissue culture plates (Griener). Lymphocytes were treated with biosynthesized AgNPs at varying doses (48–500 ug/mL) for 48 h in humidified CO2 (5% v/v). After incubation, the media were taken out and 40 uL of MTT solution per well were added. Formazan production was then allowed to occur for 4 h.MTT crystals were dissolved by adding *180 µL of DMSO per well, shaking the plates at room temperature, and measuring the absorbance at 570 nm with a microplate ELISA reader. By measuring the colorimetric* reduction of yellow MTT (3-(4, 5-dimethylthiazol-2-yl)-2, 5- diphenyl tetrazolium bromide) to purple formazan, which is dependent on mitochondria, it was possible to measure the vitality of the cells. Relative viability (%) was used to express the data, and cytotoxicity was denoted by a relative viability of less than 100%. (Hansen et al., 1989). The following equation was used to calculate relative viability (%), and the IC50 was derived using the equation for the dosage response curve.

[Absorbance of treated cells/Absorbance of control cells)] X 100

3. RESULTS AND DISCUSSION

3.1 Characterization of biosynthesized AgNPs

3.1.1 UV-Visspectroscopy

AgNPs was biosynthesized for the first-time using C. tropicalis culture supernatant and C.japonica (Kumquat) aqueous peel extract through green route approach. Reduction of Ag+ ions into AgNPs was monitored by color change and UV-Vis spectroscopy. AgNPs exhibited yellowish-brown color due to excitation of surface plasmon vibrations ***(Ibrahimet al., 2015***). In case of Kumquat aqueous peel extract (KaqPE), AgNPs were successfully biosynthesized within 12 h at room temperature under shaking incubation in darknessand within one h at 60oC under stirring conditions. Using C.tropicalis culture supernatant as a bio-reductant, the color change wasobservedforreaction mixture incubated at 45oC for 24 hat 150 rpm in darkness.Results obtained (Fig. 1), indicate that KaqPE-AgNPs require less temperature and incubation period than C .tropicalis-AgNPs.A broad absorption peak was achieved at 470 nm characteristic to KaqPE-AgNPs, while, C.tropicalis-AgNPs exhibited a well-defined resonance band at 462 nm which indicate the formation of smaller AgNPs at lower wavelength ***(Ibrahim et al., 2015)***.

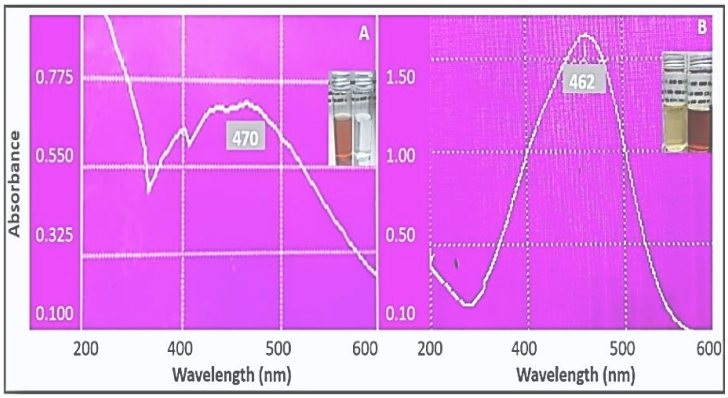

Figure (1): UV-Vis spectroscopy of Ag-NPs biosynthesized by *C. tropicalis* culture supernatant (A), and Kumquat Aqueous Peel Extract (KaqPE) (B).

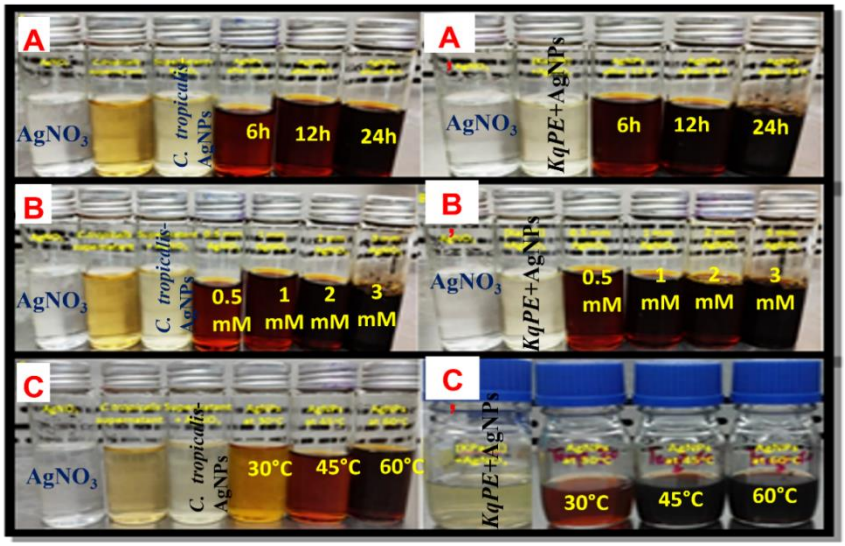

Figure (2). Effect of different incubation period on C. tropicalis-AgNPs (A), KaqPE-AgNPs (A′), effect of AgNO3 concentration on C. tropicalis-AgNPs (B), KPaqE-AgNPs (B′), effect of temperature on C. tropicalis-AgNPs (C) and KPaqE-AgNPs (C′).

The synthesis of AgNPs was optimized at different reaction conditions (**Fig. 2)** and the intensity of reddish-brown was increased with increasing the $AgNO_3$concentration, incubation time, and incubation temperature. In the case of KaqPE reaction mixture, a yellowish brown appeared with low $AgNO_3$ concentration (0.5and 1 mM) at 30^{o}C after 12 h which was rapidly converted to dark brown with increasing the incubation to 24 h and 48 h. However, *C. tropicalis*reaction mixture did not display any change in color at 30^{o}C even with increasing the Ag^+ concentration or incubation time, and the color remained yellow. Increasing the reaction mixture temperature of *C. tropicalis*to 45^{o}Cwith (1mM$AgNO_3$), the color was changed to reddish-brown after 24 h.

Increasing the reaction mixture temperature of *C. tropicalis*to 45^{o}Cwith (1mM$AgNO_3$), the color was changed to reddish-brown after 24 h.

The intensity of reddish-brown color was increased with raising the temperature to 60^{o}C and the concentration of $AgNO_3$ to 2 and 3 mM.

After48 h, the stability of reddish-brown color indicated that $AgNO_3$ was completely reduced.It is a familiar that when the reaction temperature is increased, the reactants are consumed rapidly (Park et al., 2007). Similarly, Ibrahim et al. (2015) biosynthesized AgNPs using banana peel extract and reported that the intensity of reddish-brown color indicated the formation of AgNPs that was directly proportional to temperature, incubation time, and $AgNO_3$concentration.However, adjusting the reaction mixture at pH 2.0, no color change was detected. The reddish-brown color was observed at pH values from 4.5 to 9 after incubation at 30^{o}C for 24h in darkness. Moreover, increasing the pH of reaction mixture to 9.7, 10, and 11, immediately formed reddish-brown color that was converted to deep brown after incubation under the same conditions. Results suggest that the biomolecules extracted from Kumquat peels might be inactivated under the extremely acidic conditions (pH 2.0), and thus the synthesis of AgNPs is pH dependent. Likewise, Roopan et al. (2013) studied the effect of pH on AgNPs biosynthesized using *Cocos nucifera* and showed that there is no reaction occurred at pH 2.0.

3.1.2. Transmission Electron Microscope (TEM)

TEM micrographs **(Fig.3)** confirmed the formation of spherical, monodispersed, and well distributed AgNPs with a low degree of agglomeration. The size of *C. tropicalis*-AgNPs ranged from 4 to15 nm which is smaller than KaqPE-AgNPs with average size from 8 to 20 nm. The morphology and size of biosynthesized AgNPs varies depending on the reducing agents used in the synthesis process.

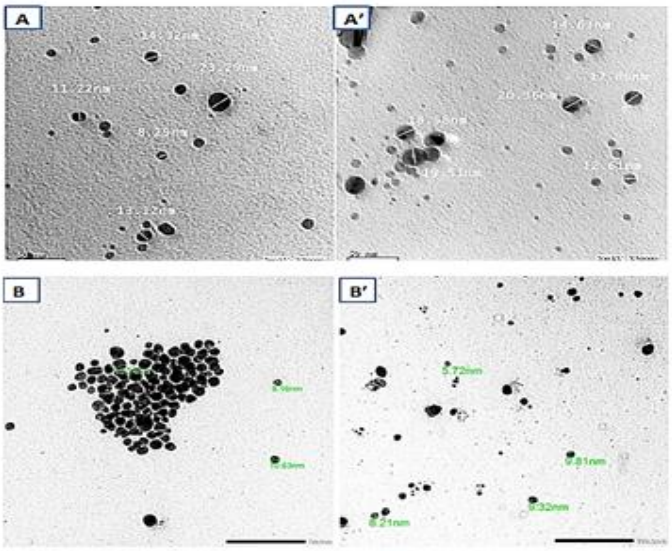

Figure (3). TEM micrographs of *C. tropicalis*-AgNPs (A, A′), and KaqPE-AgNPs (B, B′).

3.1.3. Dynamic Light scattering (DLS)

The average size distribution of AgNPs was determined using DLS **(Fig.4).** Both *C .tropicalis*-AgNPs and (KaqPE)-AgNPs were poly-dispersed and have a particle size <100 nm. DLS pattern detected that *C. tropicalis*-AgNPs had a Z average diameter of 45.7 nm according to their size distributions and poly-dispersity index (PDI) of0.398. The average size of KaqPE-AgNPs was in the range of 56.75 nm and its PDI was 0.275. Relating the number % with PDI, the biosynthesized NPs were highly dispersive in aqueous medium. Similarly, Sharma et al. (2019) produced AgNPsusing And *rographis paniculata, Phyllanthus niruri*, and *Tinosporacordifolia* plant extracts with average size distribution of 68.06, 28.38, and 37.10 nm, respectively, measured by DLS.

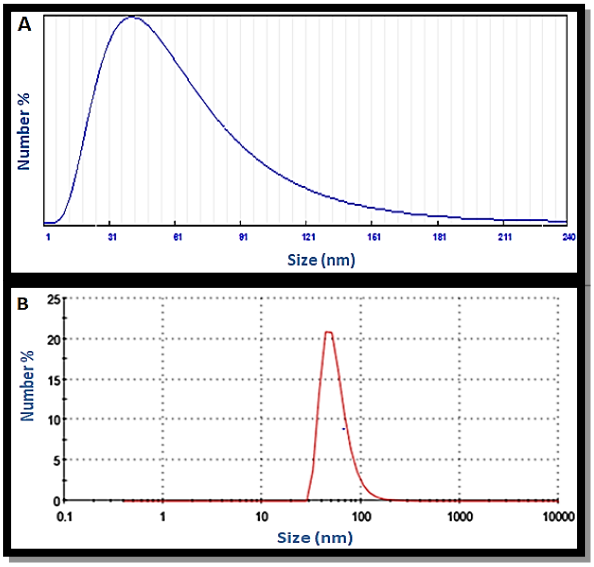

Figure (4). DLS analysis showing particle size distribution of *C. tropicalis*-Ag NPs (A) and (KaqPE)-AgNPs (B).

3.1.4. X-ray diffraction (XRD)

The XRD pattern **(Fig. 5).** of *C.tropicalis*-AgNPs exhibit characteristic intense peaks centered at 37.674º, 43.734º, and 64.277ºcorresponding to the Ag crystalline planes of 111, 200 and 220, respectively, with no impurity phases, indicating good and pure phase of AgNPs. Similar XRD diffraction peaks of KaqPE-AgNPs were exhibited at 38.003º, 49.934º, and 64.317º also corresponding to (111), (200), (220).Both XRD patterns showed these three intense peaks at 2 Θ◦values corresponding to crystallographic planes of face-centered cubic (fcc) Ag crystals and confirming that the biosynthesized AgNPs have a nano-crystalline nature.

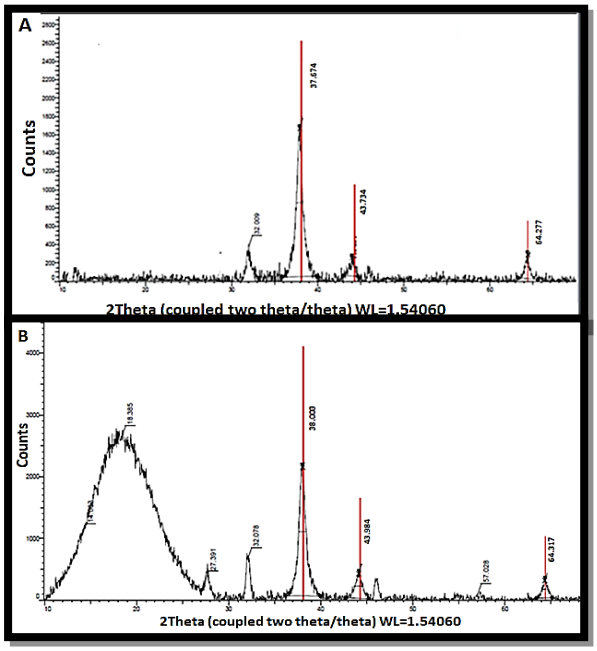

Figure (5). XRD analysis of *C. tropicalis*-Ag NPs (A), and (KaqPE)-AgNPs (B).

The intensity of peaks demonstrated the AgNPs' high degree of crystallinity (Qin et al., 2012). It's possible that additional peaks in the XRD pattern are the result of contaminants or the presence of organic biomolecules in the biological extract. Scherrer's formula was used to determine the size of AgNPs(Langford and Wilson, 1978):

$$D = K\lambda/\beta \cos\theta$$

Where **K** is the Scherrer constant with value from 0.9 to 1 (shape factor), **λ** is the X-ray wavelength (1.5418 Å), **β** is the width of the XRD peak at half-height (FWHM), and **θ** is the Bragg angle, and **D** is the grain size. Comparing the XRD spectrums with the standard sample published by the Joint Committee on Powder Diffraction Standards (file no. 04-0783) the crystalline nature of the produced AgNPs was verified (Aziz et al.,2019).

3.1.5. Energy Dispersive X-ray Spectroscopy (EDAX)

The elemental composition and the purity of the NPs have been determined using EDAX **(Fig.6).** Strong signals in the spectrum indicated the presence of Ag. Other signals from O, C, and Na atoms have also been observed mainly due to the presence of biomolecules found in *C.tropicalis* culture supernatant and KaqPEused in the biosynthesis of AgNPs.

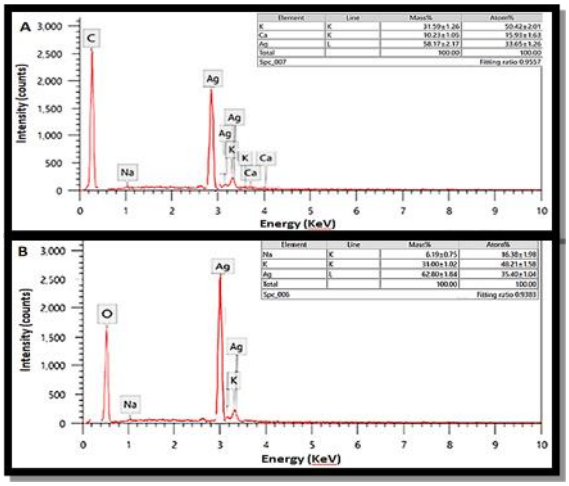

Figure (6). EDAX analysis of *C. tropicalis*-AgNPs (A), and KaqPE-AgNPs (B).

The K and Ca observed in EDAX pattern of *C.tropicalis*-AgNPs might be originated from the residual of culture medium ingredients absorbed on the NPs surface.The average atomic ratio of *C.tropicalis*-AgNPs and KaqPE-AgNPs calculated from peak's quantification (excluding C and O elements), have the

values of58.17 and 62.80, respectively. EDAX spectroscopy verified the presence of elemental Ag by the optical absorption peak at 3 KeV (**Fig. 6).**

3.1.6. Fourier Transform Infrared (FTIR)

FTIR spectrum evidently indicates the biosynthesis of AgNPs by *C.tropicalis* and KaqPE at array of absorbance bands from 400 to 4000 cm^{-1} **(Fig.7).** FTIR spectrum showed two bands at 3445 and 3428.43 cm^{-1}due to stretching vibration of O-H of alcohol or N-H of amines (Singh et al., 2014; Ibrahim, 2015).Several bands at 2962, 2941.42, 2884.52, and 2854 cm^{-1}were assigned to aldehydic C–H stretching (Sharma et al., 2019). Otherbands at 1635 and 1625 cm^{-1}were assigned to stretching vibration of the (N-C=O amide I) of proteins (Ibrahim, 2015). The bands at 1446 and 1428 cm^{-1} can be assigned to absorption

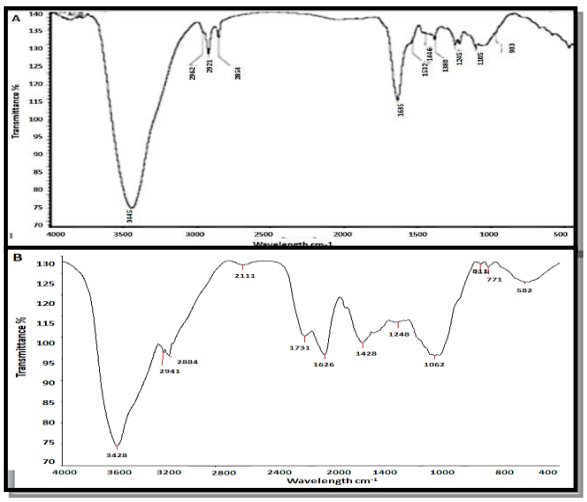

peaks of (-C-H) or (-CH_2) (Kannan *et al*., 2013).

Figure (7). FTIR analysis of biosynthesized *C. tropicalis*-Ag NPs (A), and KaqPE-AgNPs (B).

Also, the bands at 1243 and 1245$cm^{-1}$are assigned to absorption peaks of C-O-C bonds (Kannan et al., 2013; Mourdikoudis et al., 2018). bonds (Kannan et al., 2013; Mourdikoudis et al., 2018). The two spectraappeared in strong transmission bands at 1532 cm^{-1} and 1105 cm^{-1} observed in FTIR spectrum of *C.tropicalis*-AgNPs are corresponding to the bending vibration of secondary amines of proteins, and (-C-OH) stretching, respectively. FTIR spectrum of KaqE-AgNPs shows two absorption bands at 1731 cm^{-1} and 1062 cm^{-1} that are related to (-C=O) carboxyl group and (-C-N-), respectively (Ghaseminezhad et al., 2012; Mourdikoudis et al., 2018).The above bonds commonly occur in proteins which increases the stability of the biosynthesized AgNPs (Kannan et al., 2013). Overall results **(Fig. 7)** demonstrated that effective stabilizing and/or reducing agents in the two biological extractsare due to the existence of important functional groups, such as O-H, N-H, C-N, C-H, C-O-C, C-NH_2 and C=O.

3.2 Antimicrobial activity

Biosynthesized *C. tropicalis*-AgNPs and KaqPE-AgNPs were examined against different multidrug-resistant Gram positive (*L.monocytogenes*, *S. aureus*), and Gram-negative bacteria (*E. coli*, *K.pneumonia*, *A.baumannii*) and *Candida* sp. yeast **(Fig.8)**.

Biosynthesized AgNPs displayed excellent antimicrobial activity against tested microorganismsas compared to Ceftriaxone antibiotic (30µg/disc), while *C.tropicalis* culture supernatant and KaqPE didn't show any antimicrobial activity when tested as controls **(Fig.9).**

It is clear that *C. tropicalis*-AgNPs exhibited higher antimicrobial activity than KaqPE-AgNPs against all tested strains as estimated by zone of inhibition (ZOI) diameter. Results **(Table 1)** indicated that maximum antibacterial activity of *C. tropicalis*-AgNPs was against Gram-negative *K.pneumonia* with33±0.5 mm ZOI. While, KPaqE-AgNPsexhibited ZOI (31±0mm) against the same pathogen.

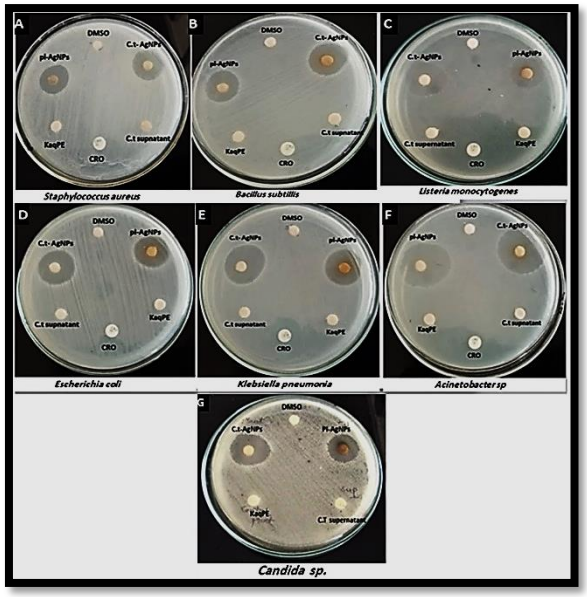

Figure (8). Antimicrobial activity of biosynthesized AgNPs, Ceftriaxone, *C. tropicalis* supernatant and KaqPE against different pathogenic strains, *E. coli* (A), *Acinetobacter* sp. (B), *K. pneumonia* (C), *S. aureus* (D), *B. subtilis* (E), *L. monocytogenes* (F), and *Candida* sp. (G).

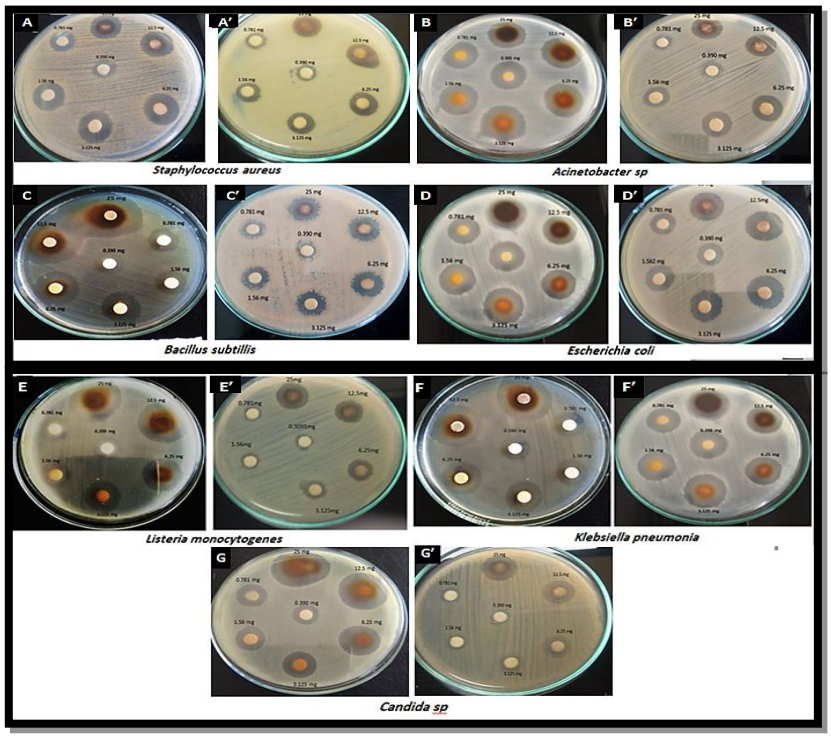

Figure (9). Antimicrobial activity of two-folds concentration of *C. tropicalis*-AgNPs (A, B, C, D, E, F, G) and KaqPE-AgNPs (A′, B′, C′, D′, E′, F′, G′) against different pathogenic bacterial and fungal strain.

Table (1). Antimicrobial activity of Ag-NPs biosynthesized by *C. tropicalis* and KaqPE, compared to Ceftriaxone antibiotic as a positive control, and negative controls (*C. tropicalis*, KaqPE, and DMSO), expressed as zone of inhibition in mm.

Strain	Zone of inhibition (mm)					
	***C. tropicalis* -AgNPs**	***C. tropicalis* supernatant**	**Plant -AgNPs**	**KaqPE**	**Cefterixone**	**DMSO**
Staphylococcus aureus	25±0.3	0±0	23.33±0.0	0±0	0±0	0±0
Bacillus subtilis	28±0.0	0±0	27±0.0	0±0	0±0	0±0
Listeria monocytogenes	27±0.3	0±0	25.66±0.3	0±0	0±0	0±0
Klebsiella pneumonia	33±0.5	0±0	31±0.0	0±0	0±0	0±0
E. coli	28.3±0.3	0±0	27±0.3	0±0	0±0	0±0
Acinetobacter sp.	29.6±0.6	0±0	27.33±0.3	0±0	0±0	0±0
***Candida sp*.**	29±0.0	0±0	24.33±0.3	0±0	ND	0±0

The diameter of ZOI increased while increasing the concentration of AgNPs **(Table 1).** Maximum antimicrobial activity of *C.tropicalis*-AgNPs was exhibited against *K. pneumonia* with a maximum ZOI(33±0.3mm)at highest concentration tested (25 mg/ml), and (17±0.3 mm) at lowest concentration (0.39mg/mL) tested. On the other hand, KPaqE-AgNPs also exhibited better antibacterial activity against *K. pneumonia* with a maximum ZOI (28±0.5mm) at 25mg/mL, and (12±0 mm) at lowest concentration. Despite the simplicity and low cost of diffusion methods, they are not always a reliable method for detecting antimicrobial activity, particularly for insoluble antimicrobial chemicals like AgNPs. Since disc diffusion is only considered a preliminary test for evaluating the bioactivity of antimicrobial drugs, additional assessment procedures were required to establish MIC.

3.3 Determination of MIC and MBC

In 96-well microtiter plates, MIC and MBC of AgNPs were carried out using conventional broth microdilution techniques (Fig. 10 and Table 2). The broth microdilution approach outperforms all other screening techniques in terms of efficiency, cost, and sensitivity. Therefore, most suited for quick quantitative analysis. The MIC was the same or lower when using the microdilution method compared to other dilution methods (Klannik et al., 2010).

Table (2). MIC and MBC values (µg/mL) of biosynthesized Ag-NPs by *C. tropicalis* and KaqPE against pathogenic bacterial and fungal strains.

MIC and MBC (µg/mL)				
Pathogenic strain	**Microbial-AgNPs**		**Plant-AgNPs**	
	MIC	**MBC**	**MIC**	**MBC**
Staphylococcus aureus	24	48	97	97
Listeria monocytogenes	48	48	195	195
Klebsiella pneumonia	24	24	48	48
E. coli	12	24	24	48
Acinetobacter sp.	12	24	24	24
Candida sp.	48	48	195	195

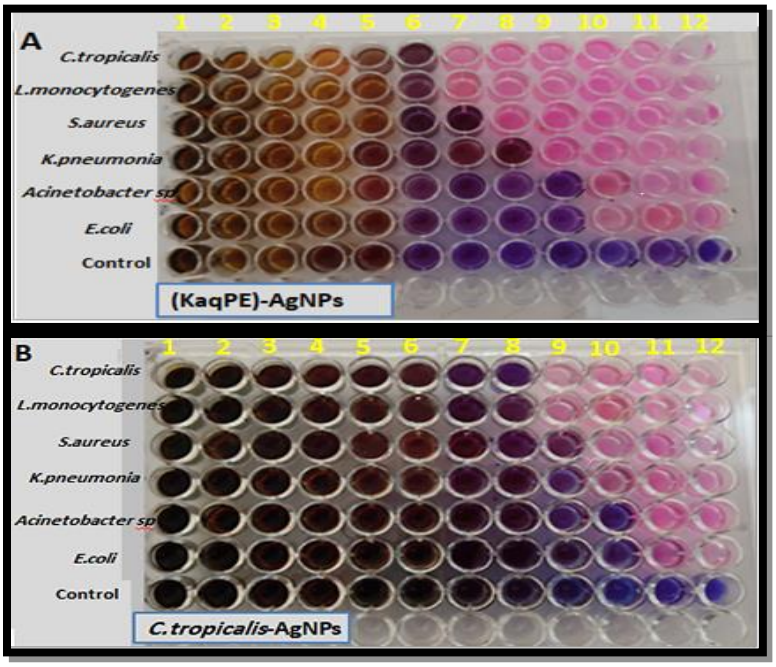

Figure (10). Determination of MIC concentration of biosynthesized Ag-NPs against pathogenic strains using Rezasurin microtiter-plate at two-folds concentration; columns from 1 to 11 contain concentrations from 6250 to 6 µg/mL, and column 12 contains bacterial suspension of each isolate as a positive control.

Resazurin dye was used in this assay as an indicator for the determination of cell growth (Fig. 10). For metabolic and viability studies, rezasurin (7-hydroxy-3H-phenoxazin-3-one 10-oxide) is typically employed (Präbst et al., 2017). Dehydrogenases and oxidoreductases that are NADPH-dependent reduce it. Resazurin changes colour as the amount of dissolved oxygen in the surrounding medium decreases as a result of bacterial acid generation and dissolved oxygen depletion (Heller and Edelblute, 2018). There are two steps to reduction. Blue resazurin is irreversibly converted to pink resorufin in the first stage. Resorufin is reversibly converted to color less dihydroresorufin in the second stage. Rezasurin has thus been incorporated into numerous anaerobe media due to its ability to change colour when oxygen is present and becoming colorless when dissolved oxygen is not present. (Mann and Markham,1998). Resazurin has many advantages as an MIC endpoint indicator because color change occurs at cell densities expressive for MIC determination (Loo et al., 2018).

The MIC value was established as the lowest concentration of AgNPs that prevented the tested bacteria from growing visibly on the microplates while maintaining the color of the resazurin indicator as blue. MBC is the lowest concentration of AgNPs to kill the bacteria that did not show any microbial growth when plated on agar media. MIC and MBC values of C. tropicalis-AgNPsagainst the studied pathogenic strains ranged from 12 µg/mL for E.coli and A. baumanniiwith MBC of 24 and48 µg/mL against Candida sp. and L. monocytogenes, respectively (Table 2 and Fig. 10). The highest MIC and MBC for KaqPE-AgNPs were also observe dagainst Candida sp .and L. monocytogenes (195 µg/mL), while A. baumanniiand E.coli showed lower MIC of 24 µg/mL,and MBC of 24 µg/mL and 48 µg/mL, respectively. However, MIC values of 24 and 97 µg/mL against S. aureus was obtained for AgNPs

biosynthesized by C. tropicalis and KaqPE, respectively. Overall results indicated that C. tropicalis-AgNPs displayed better biocidal action than KaqPE-AgNPs against L. monocytogenes, and both biosynthesized AgNPs exhibited antimicrobial efficacy against all studied-multidrug resistant strains. The results also revealed that Gram-negative strains were more susceptible to biosynthesized AgNPs than Gram-positive strains and Candida sp.

Similarly, Ibrahim et al. (2015) reported that banana-peel extract biosynthesized-AgNPs having average size of 23.7 nm had higher antimicrobial activity towards the Gram-negative E. coli (17 mm) and P. aeruginosa (20mm), as compared to Gram-positive B. subtilis (12mm) and S. aureus (16mm) probably due to the cell wall difference. Where, Gram-positive bacterial cell wall has thick multilayers of peptidoglycan protein and molecules of teichoic acids/ lipoteichoic acids making the cell wall much thicker than Gram-negative bacteria (Erjaee et al., 2017). Interestingly, Sondi and Salopek-Sondi (2004) showed effective antibacterial activity of AgNPs of average size12.4±4.2 nm against E. coliand reported that even at higher concentration of 100 μg/mL, no complete growth inhibition for an initial cell concentration of 106 CFU/mL, but only delayed the growth of E. coli. In our study ,the biosynthesized AgNPs by C. tropical is or KaqPE had average size from 4 to 20 nm and displayed MIC values of 24 μg/mL and 48 μg/mL, respectively, against E. coli with initial bacterial cell concentration of 106 CFU/mL(Table 2 and Fig. 10).

3.4 Effect of biosynthesized AgNPs on bacterial cell morphology

SEM micrographs (Fig. 11) show remarkable alterations in the morphology of treated bacterial cells as compared to untreated control after 3- 6h of incubation with AgNPs. SEM micrographs showed that the surface of untreated of L. monocytogenesor K. pneumonia was smooth, intact with typical characters of native cells surface. After 3h of exposure to MBC concentrations of C. troplicalis-AgNPs, Each bacterial cells was shrunk and dehydrated, disorganized and had a fractured membrane. However, after 3 h exposure to KaqPE-AgNPs, some of treated cells kept their native shape with intact surface as control, while some others appeared tiny and shrunk with many pits (Fig. 11).

After 6 h of treatment, all treated cells were lysed and disrupted completely; showing leakage and were completely fragmented. The entire treated cells had lost all of their metabolic functions completely. The findings unambiguously show that C. tropicalis-AgNPs mediated the fastest bactericidal activity by preventing bacterial multiplication and destroying germs within 3 hours. Also, KaqPE-AgNPs displayed almost similar bactericidal efficacy, but within 6 h. This may be because the size of C. tropicalis-AgNPs was smaller than KaqPE-AgNPs. According to Raza et al. (2016), smaller sized spherical AgNPs had the greatest bactericidal effect against bacterial strains and were more efficient at wiping out bacteria than larger ones. Chemical bioagents are also restricted since many microbes have developed resistance over many generations. Because bacteria are less likely to develop resistance to metal NPs than to chemical antibiotics, the creation of AgNPs can therefore be a substitute strategy to combat multidrug-resistant germs (Loo et al., 2018).

3.5 Mechanism of biocidal activity of AgNPs

Numerous mechanisms motivate the biocidal characteristics of AgNPs against microorganisms. AgNPs can interact with microorganisms by various ways to damage them. Firstly, AgNPs can attach to

negatively charged cell surface which alter the structural integrity of the cell wall and cause physico-chemical changes in cell membranes, thus disturb important functions such as permeability, electron transport, respiration, and osmoregulation, causing extrusion of intracellular material and eventually cell death (Sondi and Salopek-Sondi, 2004; Nel et al., 2009; Su et al., 2009). SEM results indicated that the AgNPs caused a series of similar changes on L. monocytogenes and K.pneumonia (Fig. 11). The changes in the cell wall and cell membrane facilitate internalization of AgNPs inside the cell as confirmed by the formation of pits and interruption of the bacterial cell wall. Secondly, AgNPs may release Ag+ ions which attach to bacterial cells and cause further destruction, interacting with DNA, proteins, and other sulfur and phosphorus containing cell components (Nel et al., 2009; Ibrahim, 2015). This may disturb the DNA replication, causing enzymes deactivation and proteins essential for ATP synthesis (Agnihotri et al., 2014). Moreover, Ag+ ions may disturb the function of membrane-bound enzymes and disrupt the respiratory chain (Bragg and Rainnie, 1974). Consequently, AgNPs also can generate an improved biocidal effect, which is size, shape and dose-dependent (Marambio-Jones and Hoek, 2010; Ibrahim, 2015). Smaller AgNPs displayed better and faster inhibitory effect because an intrinsic large surface area is associated with the bacterial effluent as compared to larger ones. Therefore, smaller particles released more Ag+ ions than larger ones and give better bactericidal effect (Pal et al., 2007). Likewise, Raza et al. (2016) examined the antibacterial activity of chemically prepared-AgNPs against E. coli and P. aeruginosa. Smallest spherical AgNPs established higher antibacterial activity towards both strains as compared to larger triangular or spherical AgNPs.

3.6 Cytotoxicity of the biosynthesized AgNPs

The cytotoxic activity of AgNPs against cancer cell lines (Hepatocellular carcinoma and Lung cancer) and normal cell lines (Human Skin Fibroblast) was performed by SRB assay and on Peripheral Blood Lymphocytes using MTT assay (Fig. 12). Both assays gave equivalent results in drug sensitivity testing of cancer and normal cell lines (Skehan et al., 1990). The SRB assayis used to determine cell density, by measuring cellular protein content (Vichai and Kirtikara, 2006; Vajrabhaya and Korsuwannawong, 2018).

SRB assay (Fig. 12) revealed that C. tropicalis-AgNPs exhibited cytotoxic effect against A549 and Hep-G2 with calculated IC50 of 289 and 59.5 µg/mL, respectively. While IC50 of KaqPE-AgNPs against A549 and Hep-G2 were >300 and 87.5 µg/mL, respectively. This means that C. tropicalis-AgNPs have better anticancer effect on Hep-G2 cell lines than KaqPE-AgNPs. Moreover, C. tropicalis-AgNPs exhibited cytotoxic effect against HSF cell lines having IC50 of 69.9 µg/mL, while KaqPE-AgNPs did not show any visible cytotoxicity to HSF cells at all tested concentration with IC50>300 µg/mL (Fig. 12).

Furthermore, MTT assay on Blood Lymphocytes showed higher IC50 of 2843 and 6841.6 µg/mL for C. tropicalis-AgNPs and KaqPE-AgNPs, respectively (Fig.12).This means that KaqPE-AgNPs has no harmful effect on normal HSF and Lymphocytes with cell viability (>90%) at all concentrations. The difference in cytotoxic effect of C. tropicalis-AgNPs and KaqPE-AgNPs might be due to difference in NPs size and capping agents found in the two biological extracts. Researchers suggested that potential cytotoxic effect of AgNPs depends on several factors, such as administration routes and/or NPs characteristics like size, concentration,

aggregation, exposure time, as well as capping agent used for NPs stabilization (Niska et al., 2016; Tayel et al., 2017).In the same respect, Liu et al. (2010) tested the cytotoxic effect of different sizes of AgNPs against four cancer cell lines namely, HepG-2, A549 (human lung adenocarcinoma ephithelial cells), SGC-7901 (human stomach cancer cells), and MCF7 (human breast adenocarcinoma cells),and reported that5 nm sized AgNPs was more cytotoxic, followed by 50 nm sized AgNPs with higher IC50. On the other hand, plant extracts contain many bioactive phytocompounds, such as, flavonoids, phenols, and alkaloids, which acts as capping agents for the stabilizing AgNPs, therefore, not only the presence of capping agents of NPs, but also its type affects the cytotoxicity (Fahmy et al., 2019).Interestingly, Selvan et al. (2018) biosynthesized AgNPs using garlic, green tea, and turmeric extracts, and tested their cytotoxic effect compared to chemically synthesized ones on breast adenocarcinoma (MCF-7), cervical (HeLa), epithelioma (Hep-2), lung cancer (A549), and normal human dermal fibroblasts (NHDF) cell linesusing MTT assay. Selvanet al. (2018) described that biosynthesized AgNPs exhibited higher IC50 values against normal NHDF with IC50>100 µg/mL, which indicates their lower toxicity for normal cell lines. However, biosynthesized AgNPs exhibits higher cytotoxicity against cancer cell lines (MCF-7, A549, Hep-2, and Hela). Bio-mediated AgNPs using turmeric extract had highest cytotoxicity because ofhigh phytocompounds content in turmeric extract. Thus, the difference in cytotoxic effect of biosynthesized AgNPs returns to the difference in capping agents found in different plant extracts (Selvan et al., 2018). In addition, Paknejadi et al. (2018) assessed the cytotoxicity of chemically prepared AgNPson normal HSF by testing the same concentrations used againstthe skin pathogen Candida sp.,which exhibited IC50 values of 30.64 and 14.98 µg/mL after 24 and 48h, respectively.

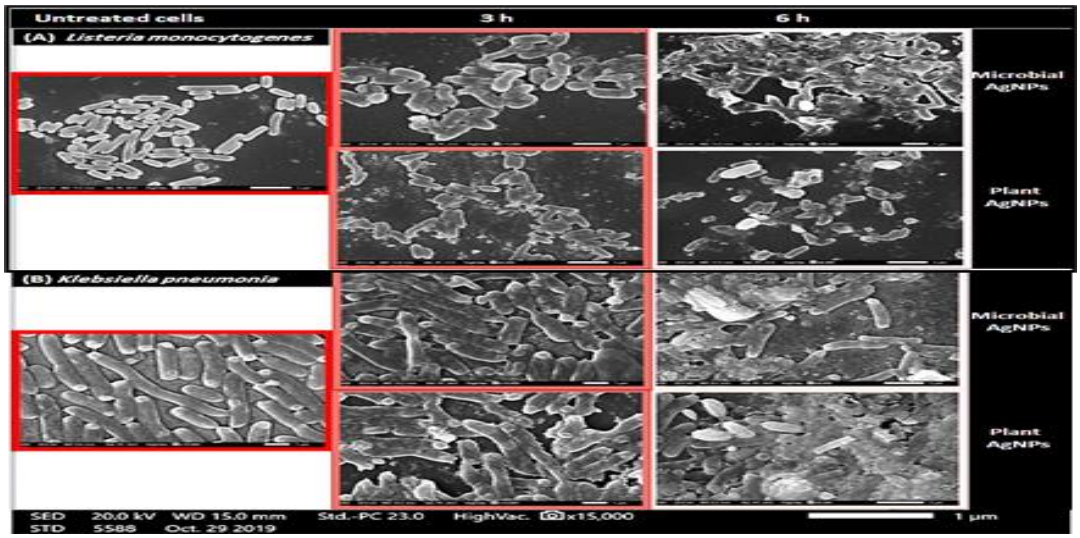

Figure (11). SEM micrograph showing the effect of biosynthesized AgNPs on cellular morphology of Listeria monocytogenes (A), and Klebsiella pneumonia treated by MBC concentration after 3 and 6 h of incubation.

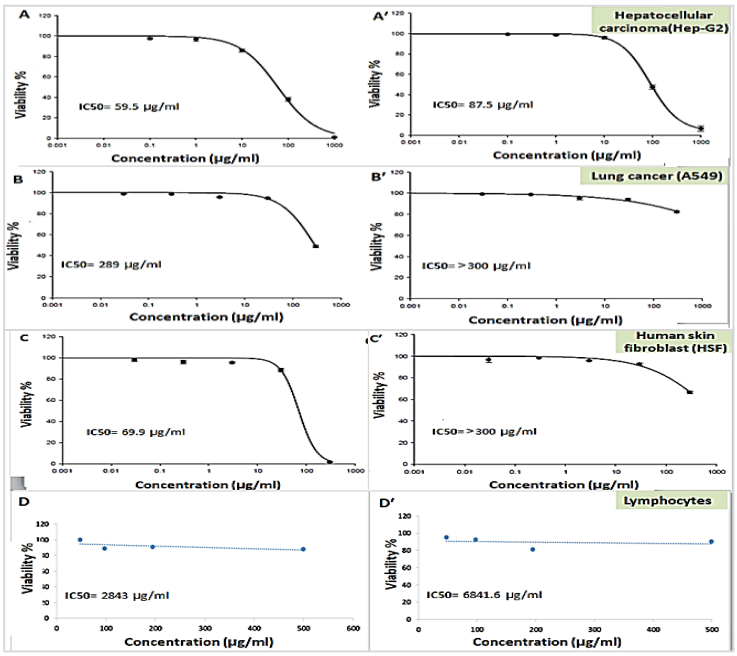

Figure (12). Cytotoxic effect of Ag-NPs biosynthesized by C. tropicalis (A, B, C, D) and Kumquat extract (A′, B′, C′, D′) against cancer cell lines (Hep-G2 and Lung cancer), HSF normal cell lines using SRB assay, and Blood Lymphocytes using MTT assay, data expressed as the mean value of cell viability (% of control) ± S.D and IC50 was calculated.

Our results (Fig. 12)investigated green biosynthesized AgNPs that exhibited less cytotoxic effect when tested on HSFthan those chemically prepared by Paknejadi et al. (2018) with IC50 of 69.9 and >300 µg/mL for C. tropicalis-AgNPs and KaqPE-AgNPs, respectively, and also exhibited better antimicrobial activity against Candida sp. asskin pathogen. The lower cytotoxicity of biosynthesized AgNPs is probably due to the bioactive molecules in the bio-source used for synthesis and capping, being verified by FTIR. Overall, both biosynthesized AgNPs showed significantly higher IC50 than its MBC values against all tested pathogens. Consequently, they are safe and effective antimicrobial agent for industrial, cosmetics and medical applications.

5. CONCLUSION

A comparative study for the bio-mediation of AgNPs synthesis via novel green method has been investigated. AgNPs were successfully biosynthesized extracellularly by C. tropicalis culture supernatant and C. japonica peels (KaqPE). KaqPE is efficiently used as natural, renewable, and low-cost bio-reducing agent for AgNPs synthesis in a high yield after 12h at room temperature. The biosynthesized AgNPs exhibited excellent antibacterial activity against different multidrug-resistant Gram-positive (L. monocytogenes), Gram-negative (Acinetobacter baumannii, E. coli, K. pneumonia)isolates, and Candida sp. The results revealed that Gram-negative were more susceptible to AgNPs than Gram-positive and Candida sp. due to different cell wall. SEM micrographs showed complete cell destruction ofK. pneumonia and L. monocytogenesafter 6h of exposure to MBC values of AgNPs. The cytotoxic

effect of bio mediated AgNPs was evaluated against normal cell lines as HSF and Blood Lymphocytes which exhibited IC50 higher than its MBC values against studied pathogens. In conclusion, bio mediated AgNPs in the present study can be considered safe for usage as antimicrobial bioagent in many applications

6. REFERENCES

Agnihotri, S., Mukherji, S., & Mukherji, S. (2014). Size-controlled silver nanoparticles synthesized over the range 5–100 nm using the same protocol and their antibacterial efficacy. Rsc Advances, 4(8), 3974-3983.

Ahmed, S., Ahmad, M., Swami, B. L., & Ikram, S. (2016). A review on plants extracts mediated synthesis of silver nanoparticles for antimicrobial applications: a green expertise. Journal of advanced research, 7(1), 17-28.

Aziz, S. B., Hussein, G., &Brza, M. A. (2019). J. Mohammed S, T. Abdulwahid R, Raza Saeed S, et al. Fabrication of Interconnected Plasmonic Spherical Silver Nanoparticles with Enhanced Localized Surface Plasmon Resonance (LSPR) Peaks Using Quince Leaf Extract Solution.

Bragg, P.D.; Rainnie, D.J. The effect of silver ions on the respiratory chains of Escherichia coli. Can. J. Microbiol. 1974, 20, 883–889

Clinical and Laboratory Standards Institute. (2012). Methods for dilution antimicrobial susceptibility tests for bacteria that grow aerobically, approved standard. CLSI document M07-A9, 32.

El-Baz, A. F., Shetaia, Y. M., &Elkhouli, R. R. (2011). Xylitol production by Candida tropicalis under different statistically optimized growth conditions. African Journal of Biotechnology, 10(68), 15353-15363.

Erjaee, H., Rajaian, H., &Nazifi, S. (2017). Synthesis and characterization of novel silver nanoparticles using Chamaemelum nobile extract for antibacterial application. Advances in Natural Sciences: Nanoscience and Nanotechnology, 8(2), 025004.

Fahmy, H. M., Mosleh, A. M., Abd Elghany, A., Shams-Eldin, E., Serea, E. S. A., Ali, S. A., &Shalan, A. E. (2019). Coated silver nanoparticles: Synthesis, cytotoxicity, and optical properties. RSC advances, 9(35), 20118-20136.

Fischer, E.R., Hansen, B.T., Nair, V., Hoyt, F.H., Dorward, D.W.(2012). Scanning electron microscopy. CurrProtocMicrobiol. May;Chapter 2:Unit 2B.2.. doi: 10.1002/9780471729259.mc02b02s25.

Ghaseminezhad, S. M., Hamedi, S., &Shojaosadati, S. A. (2012). Green synthesis of silver nanoparticles by a novel method: Comparative study of their properties. Carbohydrate polymers, 89(2), 467-472.

Hansen, M. B., Nielsen, S. E., & Berg, K. (1989). Re-examination and further development of a precise and rapid dye method for measuring cell growth/cell kill. Journal of immunological methods, 119(2), 203-210.

Heller, L. C., & Edelblute, C. M. (2018). Long-term metabolic persistence of Gram-positive bacteria on health care-relevant plastic. American journal of infection control, 46(1), 50-53.

Ibrahim, H. M. (2015). Green synthesis and characterization of silver nanoparticles using banana peel extract and their antimicrobial activity against representative microorganisms. Journal of Radiation Research and Applied Sciences, 8(3), 265-275.

Kannan, R. R. R., Stirk, W. A., & Van Staden, J. (2013). Synthesis of silver nanoparticles using the seaweed Codium capitatum PC Silva

(Chlorophyceae). South African Journal of Botany, 86, 1-4.

Kizhakeyil, A., Ong, S. T., Fazil, M. H. U. T., Chalasani, M. L. S., Prasannan, P., & Verma, N. K. (2019). Isolation of human peripheral blood T-lymphocytes. In T-Cell Motility (pp. 11-17). Humana Press, New York, NY.

Klančnik, A., Piskernik, S., Jeršek, B., &Možina, S. S. (2010). Evaluation of diffusion and dilution methods to determine the antibacterial activity of plant extracts. Journal of microbiological methods, 81(2), 121-126.

Langford, J. I., & Wilson, A. J. C. (1978). Scherrer after sixty years: a survey and some new results in the determination of crystallite size. Journal of applied crystallography, 11(2), 102-113.

Liu, W., Wu, Y., Wang, C., Li, H. C., Wang, T., Liao, C. Y., ... & Jiang, G. B. (2010). Impact of silver nanoparticles on human cells: effect of particle size. Nanotoxicology, 4(3), 319-330.

Loo, Y. Y., Rukayadi, Y., Nor-Khaizura, M. A. R., Kuan, C. H., Chieng, B. W., Nishibuchi, M., & Radu, S. (2018). In vitro antimicrobial activity of green synthesized silver nanoparticles against selected Gram-negative foodborne pathogens. Frontiers in microbiology, 9, 1555.

Mann, C. M., & Markham, J. L. (1998). A new method for determining the minimum inhibitory concentration of essential oils. Journal of applied microbiology, 84(4), 538-544.

Marambio-Jones, C., & Hoek, E. M. (2010). A review of the antibacterial effects of silver nanomaterials and potential implications for human health and the environment. Journal of nanoparticle research, 12(5), 1531-1551.

Morones, J. R., Elechiguerra, J. L., Camacho, A., Holt, K., Kouri, J. B., Ramírez, J. T., &Yacaman, M. J. (2005). The bactericidal effect of silvernanoparticles. Nanotechnology, 16 (10), 2346.

Mourdikoudis, S., Pallares, R. M., & Thanh, N. T. (2018). Characterization techniques for nanoparticles: comparison and complementarity upon studying nanoparticle properties. Nanoscale, 10(27), 12871-12934.

Nel, A. E., Mädler, L., Velegol, D., Xia, T., Hoek, E. M., Somasundaran, P., ... & Thompson, M. (2009). Understanding biophysicochemical interactions at the nano–bio interface. Nature materials, 8(7), 543-557.

Niska, K., Knap, N., Kędzia, A., Jaskiewicz, M., Kamysz, W., &Inkielewicz-Stepniak, I. (2016). Capping agent-dependent toxicity and antimicrobial activity of silver nanoparticles: an in vitro study. Concerns about potential application in dental practice. International journal of medical sciences, 13(10), 772.

Paknejadi, M., Bayat, M., Salimi, M., &Razavilar, V. (2018). Concentration-and time-dependent cytotoxicity of silver nanoparticles on normal human skin fibroblast cell line. Iran Red Crescent Med J, 20(10).

Pal, S., Tak, Y. K., & Song, J. M. (2007). Does the antibacterial activity of silver nanoparticles depend on the shape of the nanoparticle? A study of the Gram-negative bacterium Escherichia coli. Applied and environmental microbiology, 73(6), 1712-1720.

Park, J., Joo, J., Kwon, S. G., Jang, Y., & Hyeon, T. (2007). Synthesis of monodisperse spherical nanocrystals. AngewandteChemie International Edition, 46(25), 4630-4660.

Pourali, P., &Yahyaei, B. (2016). Biological production of silver nanoparticles by soil isolated bacteria and preliminary study of their cytotoxicity and cutaneous wound healing efficiency in rat. Journal of

Trace Elements in Medicine and Biology, 34, 22-31.

Präbst, K., Engelhardt, H., Ringgeler, S., &Hübner, H. (2017). Basic colorimetric proliferation assays: MTT, WST, and resazurin. In Cell viability assays (pp. 1-17). Humana Press, New York, NY.

Qin, D. Z., Yang, G., He, G. X., Zhang, L. I., Zhang, Q. X., & Li, L. Y. (2012). The investigation on synthesis and optical properties of Ag-doped ZnS nanocrystals by hydrothermal method. Chalcogenide Lett, 9(11), 441-446.

Raza, M. A., Kanwal, Z., Rauf, A., Sabri, A. N., Riaz, S., & Naseem, S. (2016). Size-and shape-dependent antibacterial studies of silver nanoparticles synthesized by wet chemical routes. Nanomaterials, 6(4), 74.

Reenaa, M., & Menon, A. S. (2017). Synthesis of silver nanoparticles from different citrus fruit peel extracts and a comparative analysis on its antibacterial activity. International Journal of Current Microbiology and Applied Sciences, 6(7), 2358-2365.

Roopan, S. M., Madhumitha, G., Rahuman, A. A., Kamaraj, C., Bharathi, A., & Surendra, T. V. (2013). Low-cost and eco-friendly phyto-synthesis of silver nanoparticles using Cocos nucifera coir extract and its larvicidal activity. Industrial Crops and Products, 43, 631-635.

Selvan, D. A., Mahendiran, D., Kumar, R. S., &Rahiman, A. K. (2018). Garlic, green tea and turmeric extracts-mediated green synthesis of silver nanoparticles: Phytochemical, antioxidant and in vitro cytotoxicity studies. Journal of Photochemistry and Photobiology B: Biology, 180, 243-252.

Shamaila, S., Sajjad, A. K. L., Farooqi, S. A., Jabeen, N., Majeed, S., & Farooq, I. (2016). Advancements in nanoparticle fabrication by hazard free eco-friendly green routes. Applied Materials Today, 5, 150-199.

Sharma, V., Kaushik, S., Pandit, P., Dhull, D., Yadav, J. P., & Kaushik, S. (2019). Green synthesis of silver nanoparticles from medicinal plants and evaluation of their antiviral potential against chikungunya virus. Applied microbiology and biotechnology, 103(2), 881-891.

Singh, K., Panghal, M., Kadyan, S., & Yadav, J. P. (2014). Evaluation of antimicrobial activity of synthesized silver nanoparticles using Phyllanthus amarus and Tinospora cordifolia medicinal plants. Journal of Nanomedicine & Nanotechnology, 5(6), 1.

Singla, R., Guliani, A., Kumari, A., & Yadav, S. K. (2016). Metallic nanoparticles, toxicity issues and applications in medicine. In Nanoscale materials in targeted drug delivery, theragnosis and tissue regeneration (pp. 41-80). Springer, Singapore.

Skehan, P., Storeng, R., Scudiero, D., Monks, A., McMahon, J., Vistica, D., ... & Boyd, M. R. (1990). New colorimetric cytotoxicity assay for anticancer-drug screening. JNCI: Journal of the National Cancer Institute, 82(13), 1107-1112.

Sondi, I., &Salopek-Sondi, B. (2004). Silver nanoparticles as antimicrobial agent: a case study on E. coli as a model for Gram-negative bacteria. Journal of colloid and interface science, 275(1), 177-182.

Srikar, S. K., Giri, D. D., Pal, D. B., Mishra, P. K., & Upadhyay, S. N. (2016). Green synthesis of silver nanoparticles: a review. Green and Sustainable Chemistry, 6(01), 34.

Su, H. L., Chou, C. C., Hung, D. J., Lin, S. H., Pao, I. C., Lin, J. H., et al. (2009). The disruption of bacterial membrane integrity through ROS generation induced by nanohybrids of silver and clay. Biomaterials, 30, 5979e5987.

Tayel, A. A., Sorour, N. M., El-Baz, A. F., & Wael, F. (2017). Nanometals appraisal in food preservation and food-related activities. In Food Preservation (pp. 487-526). Academic Press.

Vajrabhaya, L. O., &Korsuwannawong, S. (2018). Cytotoxicity evaluation of a Thai herb using tetrazolium (MTT) and sulforhodamine B (SRB) assays. Journal of Analytical Science and Technology, 9(1), 1-6.

Valgas, C., Souza, S. M. D., Smânia, E. F., &Smânia Jr, A. (2007). Screening methods to determine antibacterial activity of natural products. Brazilian journal of microbiology, 38(2), 369-380.

Vichai, V., &Kirtikara, K. (2006). Sulforhodamine B colorimetric assay for cytotoxicity screening. Nature protocols, 1(3), 1112-1116.

Zhang, X. F., Liu, Z. G., Shen, W., &Gurunathan, S. (2016). Silver nanoparticles: synthesis, characterization, properties, applications, and therapeutic approaches. International journal of molecular sciences, 17(9), 1534.